

# Journal of Materials Chemistry C

Accepted Manuscript



This is an *Accepted Manuscript*, which has been through the Royal Society of Chemistry peer review process and has been accepted for publication.

*Accepted Manuscripts* are published online shortly after acceptance, before technical editing, formatting and proof reading. Using this free service, authors can make their results available to the community, in citable form, before we publish the edited article. We will replace this *Accepted Manuscript* with the edited and formatted *Advance Article* as soon as it is available.

You can find more information about *Accepted Manuscripts* in the [Information for Authors](#).

Please note that technical editing may introduce minor changes to the text and/or graphics, which may alter content. The journal's standard [Terms & Conditions](#) and the [Ethical guidelines](#) still apply. In no event shall the Royal Society of Chemistry be held responsible for any errors or omissions in this *Accepted Manuscript* or any consequences arising from the use of any information it contains.

## ARTICLE

# Triple-signaling mechanisms-based three-in-one multi channel chemosensor for discriminating $\text{Cu}^{2+}$ , acetate and ion pair mimicking AND, NOR, INH and IMP logic functions

Cite this: DOI: 10.1039/x0xx00000x

Received 00th January 2012,  
Accepted 00th January 2012

DOI: 10.1039/x0xx00000x

www.rsc.org/

Prabhpreet Singh<sup>a,\*</sup>, Harminder Singh<sup>a</sup>, Gaurav Bhargava<sup>b</sup> and Subodh Kumar<sup>a</sup>

Chemosensor **1** shows three different responses towards  $\text{Cu}^{2+}$ , acetate and  $\text{Cu}(\text{OAc})_2$  ion pair at different wavelengths independently, in its absorption and fluorescence behaviour following triple-signaling mechanisms such as internal charge transfer (ICT), C=N rotation and excited state intramolecular proton transfer (ESIPT). Chemosensor **1** shows blue shift of the absorption band from 337 nm to 308 nm in the presence of  $\text{Cu}^{2+}$  ions (ICT). It exhibits fluorescence ‘turn-off’ response at  $\lambda_{\text{em}}$  458 nm in the presence of 1 equiv. of  $\text{Cu}^{2+}$  ions. Further addition of  $\text{Cu}^{2+}$  (6 equiv.) results in ~24 times enhancement in the emission intensity at  $\lambda_{\text{em}}$  427 nm mimicking ‘ON-OFF-ON’ molecular switch (ESIPT and C=N rotation). The addition of acetate ions to solution of **1** results in red shift of the absorption band from 337 to 360 nm (ICT) and ~4 times enhancement of emission intensity at  $\lambda_{\text{em}}$  458 nm (ESIPT). On addition of  $\text{Cu}(\text{OAc})_2$  ion pair, **1** shows the apparent effect of  $\text{Cu}^{2+}$  (blue shift; 337 to 308 nm) and acetate (red shift; 337 to 380 nm) which indicates the synergistic effect of both  $\text{Cu}^{2+}$  and  $\text{AcO}^-$  on each other’s binding. The potential application of chemosensor **1** for construction of INHIBIT (INH), IMPLICATION (IMP), AND, NOR, YES and NOT logic gates using  $\text{Cu}^{2+}$  and acetate as inputs and absorbance/emission as outputs has been elaborated.

## 1. Introduction

For last few years in supramolecular chemistry, the efforts are being undertaken to develop dual chemosensors which can perform recognition of both cations and anions, presumably due to potential applications of cations and anions in the field of biochemistry, pharmaceuticals, environmental science and chemical biology.<sup>1</sup> Dual chemosensors<sup>2-7</sup> which possess colorimetric (‘naked eye’ detection) and fluorescent response for cation and anion at different wavelengths through modulation of various signaling mechanisms<sup>8</sup> are still in great demand. Although cation complexation (metal coordination) has roots quite different from anion complexation (involving hydrogen bonds, electrostatic interactions, deprotonation etc.)<sup>9</sup>, yet we have witnessed slow progress in the development of dual chemosensors to recognize combination of cation and anion.<sup>5-7</sup>

Dual chemosensor for cation and anion includes thioxanthone based dual channel for  $\text{Hg}^{2+}/\text{F}^-$ ;<sup>7a</sup> Schiff base derivatives of 1-(2-aminophenyl)-3-phenylthiourea<sup>7b</sup> and naphthyl based Schiff base<sup>7c</sup> for  $\text{Cu}^{2+}/\text{F}^-$  and chemosensor for  $\text{Cu}^{2+}$ /acetate ion.<sup>8</sup> Nitrophenyl urea appended macrocycle shows logic operation on addition of  $\text{OH}^-/\text{Cu}^{2+}$  and  $\text{F}^-/\text{Hg}^{2+}$  ions.<sup>9</sup> Moreover, in literature thio(urea) subunits are used in combination with other hydrogen bonding groups such as -NH, -OH, indole or pyrrole to execute the task of recognizing the anions.<sup>10</sup> The direct Schiff base conjugates of urea and thiourea with salicylaldehyde or naphthaldehyde have been reported for the recognition of metal ions.<sup>11-14</sup> These dual chemosensors utilize either one or combination of different signaling mechanisms such as photoinduced electron transfer (PET), internal charge transfer (ICT), excited state intramolecular proton transfer (ESIPT), inhibition of C=N rotation etc., with or without ratiometric<sup>8</sup> behavior to signal cation and anion binding. However, the combination of more than two signaling mechanisms and separate response for cation, anion and ion pair at different wavelengths by one chemosensor (3-in-1) to turn multiple absorption and emission channels independently has not been reported so far.

Among the transition metal ions, copper is considered as significant pollutant, despite being an essential element in biological systems<sup>15</sup>, whereas acetate ions find potential

<sup>a</sup>Department of Chemistry, UGC Centre for Advanced Studies, Guru Nanak Dev University, Amritsar 143 005, India. E-mail: prabhpreet.chem@gndu.ac.in; Tel: +91-84271-01534

<sup>b</sup>Department of Applied Sciences, Punjab Technical University, Kapurthala-144601, Punjab, India.

Electronic Supplementary Information (ESI) available: [Experimental details, additional photophysical studies of chemosensor **1-3** and control compounds **4-6**]. See DOI: 10.1039/c000000x/

applications in the field of pharmaceuticals, biochemistry and environmental science.<sup>16</sup> Copper acetate has been known for its use in textile, dyeing, printing, preservative for cellulose materials, as fungicide/insecticide and as a catalyst for various organic reactions. So, our environment is being continuously contaminated by copper and its compounds through industrial and natural sources. Copper is also considered as notorious quencher of fluorescence and in this context chemosensor which shows fluorescence enhancement as a result of copper ion binding are still favored.<sup>10,17</sup>

Presently, electronic engineers are facing great challenge to transform the digital information technology to the nanometer scale.<sup>18</sup> Single-molecule electronics in which “on-off”, “off-on” and “on-off-on” switching behavior at molecular level modulated by single input (proton, metal ions) has already been demonstrated when first AND logic gate was mimicked with optical signals by de Silva et al.<sup>19</sup> In subsequent years, several molecular analogs of AND, OR, NOR, XOR, INHIBIT and NAND logic gates<sup>19-21</sup> along with half subtractor, half adder, full adder and full subtractor<sup>22-25</sup> have been described. In this context, the dual chemosensors which exhibit multiple output channels are currently of particular interest because they could be used for construction of simple and complex molecular logic circuits. In our previous works, we have developed tetrapodal and dipodal systems based molecular switches and logic gates.<sup>26, 27</sup> Recently, we reported first dual chemosensor based on perylene diimide for the ratiometric detection of Cu<sup>2+</sup>/CN<sup>-</sup> ions.<sup>28</sup> Now, we propose that fluorescent Schiff base and urea subunits attached to 1,2-diaminobenzene platform would provide reasonable pre-organization to the dipodal architectures<sup>29-30</sup> and their individual interactions with cation and anion would result in different response at different wavelengths.

In this paper, we report the synthesis of chromo-fluorescent chemosensor **1** (Fig. 1) and its photophysical properties towards various cations, anions and ion pair. Chemosensor **1** presents unique and rare example of 3-in-1 molecular system where multi-channel signals were observed in the presence of Cu<sup>2+</sup>, acetate and Cu(AcO)<sub>2</sub> ion pair through modulation of triple-signaling mechanism (ICT, ESIPT and C=N rotation) at different wavelengths independently. The potential application of chemosensor **1** for construction of INH, IMP, AND, NOR, YES and NOT logic gates has been elaborated. For control experiments chemosensors **2** and **3** have been synthesized.

## 2. Experimental

### 2.1. Materials and Characterization

Chemicals and solvents were of reagent grade and used without further purification unless otherwise stated. All reactions were performed under N<sub>2</sub> atmosphere. Acetonitrile (HPLC grade) and ethanol were purchased from Spectrochem India Ltd and Changshu Yangyuan Chemical China respectively. Chromatographic purification was done with silica gel 60-120 mesh. TLC was performed on aluminium sheets coated with silica gel 60 F254 (Merck, Darmstadt). NMR spectra were recorded on Bruker and JEOL (operating at 500 and 300 for <sup>1</sup>H; 125 and 75 MHz for <sup>13</sup>C, respectively). The peak values were obtained as ppm (δ), and referenced to the TMS as reference in

<sup>1</sup>H NMR and deuterated solvent in <sup>13</sup>C NMR spectra. Abbreviations used for splitting patterns are s = singlet, bs = broad singlet, t = triplet, q = quartet, m = multiplet. Fourier transform infrared (FT-IR) spectra were recorded on Perkin Elmer 92035. The fluorescence spectra were recorded by excitation at 330 nm unless otherwise stated. The fluorescence titrations were performed on Varian Carey Eclipse fluorescence and BH Chronos spectrophotometer. The absorption spectra were recorded on Shimadzu-2450 spectrophotometer from Shimadzu. HRMS spectra were recorded on Bruker MicroToff/QII. <sup>1</sup>H NMR titration of **1** against acetate ion, Cu<sup>2+</sup> ion and Cu(OAc)<sub>2</sub> ion pair were performed in DMSO (*d*<sub>6</sub>) on 300 and 500 MHz NMR spectrometer. All the data were then processed in Top Spin software to draw the stacking spectra. Theoretical calculations were carried out using density functional theory (DFT) at B3LYP/6-31G(d,p) basis set. The solutions of chemosensor **1-3** were prepared in acetonitrile (HPLC grade). The solutions of metal perchlorates and anions as tetrabutylammonium salts were prepared in acetonitrile (HPLC grade) and were added in microliter quantities. All absorption and fluorescence scans were saved as ACSII files and further processed in Excel™ to produce all graphs shown. The spectral data were analyzed through curve fitting procedures by using non-linear regression analysis program SPECFIT 3.0.36 to determine the stability constants and the distribution of various species. The intermediate compounds **4,5**<sup>31</sup> and **6**<sup>32</sup> were synthesized after modification of the literature procedures (for synthetic detail of **4-6** see supporting information).

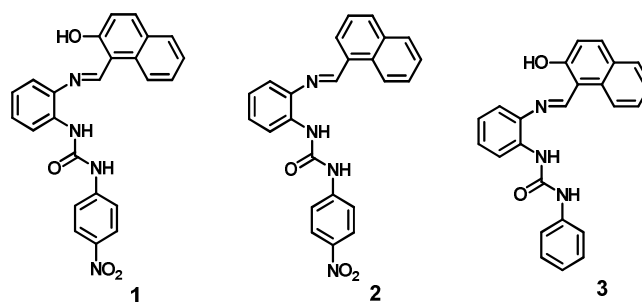


Fig. 1 Molecular structure of chemosensors 1-3.

### 2.2. Synthesis of Chemosensor 1-3

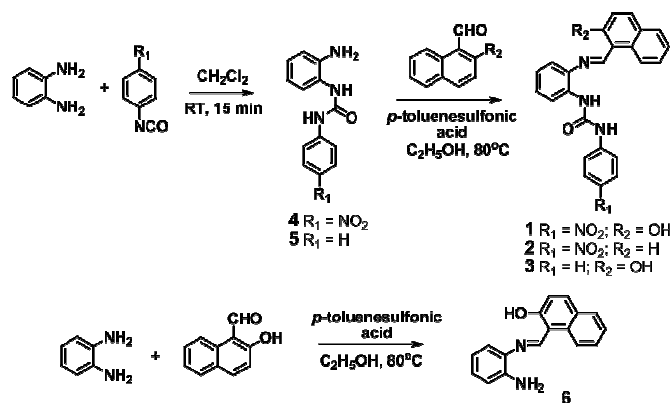
**General procedure:** To a solution of 2-hydroxy-1-naphthaldehyde (127 mg, 0.7350 mmol) in CHCl<sub>3</sub>-EtOH (1:9) mixture, 1-(2-aminophenyl)-3-(4-nitrophenyl)urea (**4**) (200 mg, 0.7350 mmol) and catalytic amount of *p*-toluenesulfonic acid were added and reaction mixture was stirred for 2h at 80°C (Scheme 1). During this time, yellow solid precipitated out in the reaction mixture. The yellow solid was filtered and washed with ethanol to isolate the pure chemosensor **1**.

**Chemosensor 1:** Yellow solid (225 mg, 72 %); m.p 272-276 °C; R<sub>f</sub> = 0.35 (50% ethyl acetate:hexane); <sup>1</sup>H NMR (500 MHz, DMSO-*d*<sub>6</sub>) δ 14.88 (s, 1H), 9.93 (s, 1H), 9.64 (s, 1H), 8.56 (d, 2H, *J* = 5 Hz), 8.19 (d, 2H, *J* = 10 Hz), 8.00 (d, 1H, *J* = 10 Hz), 7.89 (d, 1H, *J* = 5 Hz), 7.86 (d, 1H, *J* = 10 Hz), 7.71 (d, 2H, *J* = 10 Hz), 7.64 (d, 1H, *J* = 5 Hz), 7.58 (t, 1H, *J* = 5 Hz), 7.40 (t, 1H, *J* = 5 Hz), 7.32 (t, 1H, *J* = 5 Hz), 7.26 (t, 1H, *J* = 10 Hz), 7.13 (d, 1H, *J* = 10 Hz) ppm; <sup>13</sup>C NMR (125 MHz, DMSO-*d*<sub>6</sub>):

$\delta$  166.8, 159.2, 152.7, 146.8, 141.5, 139.3, 136.5, 133.3, 131.8, 129.5, 128.6, 127.5, 127.2, 125.6, 125.3, 124.1, 123.4, 121.2, 121.1, 120.2, 118.0, 110.1 ppm;  $\nu_{\max}$  (KBr)/ $\text{cm}^{-1}$ : 3435, 1665, 1611, 1560, 1533, 1504, 1459, 1342, 1331; HRMS (TOF MS ESI) calculated for  $\text{C}_{24}\text{H}_{18}\text{N}_4\text{O}_4$   $m/z$  426.1328; found 427.1352. ( $\text{M}+\text{H}^+$ ).

**Chemosensor 2:** Yellow solid (235 mg, 78 %);  $R_f = 0.40$  (30% ethyl acetate:hexane);  $^1\text{H}$  NMR (500 MHz,  $\text{DMSO}-d_6$ )  $\delta$  10.30 (s, 1H), 9.50 (s, 1H), 9.00 (d, 1H,  $J = 8$  Hz), 8.67 (s, 1H), 8.49 (d, 1H,  $J = 7$  Hz), 8.28 (d, 1H,  $J = 8$  Hz), 8.19 (t, 4H,  $J = 9.5$  Hz), 8.10 (d, 1H,  $J = 8$  Hz), 7.75-7.68 (m, 5H), 7.64 (t, 1H,  $J = 7$  Hz), 7.51 (d, 1H,  $J = 7$  Hz), 7.30 (t, 1H,  $J = 7$  Hz), 7.13 (t, 1H,  $J = 7.5$  Hz) ppm;  $^{13}\text{C}$  NMR (125 MHz,  $\text{DMSO}-d_6$ ):  $\delta$  159.5, 152.2, 146.9, 141.5, 140.1, 134.1, 133.9, 131.8, 131.7, 129.4, 129.2, 128.0, 127.6, 126.8, 126.0, 125.6, 124.4, 123.3, 119.4, 118.5, 117.9, 117.6 ppm; HRMS (TOF MS ESI) calculated for  $\text{C}_{24}\text{H}_{18}\text{N}_4\text{O}_3$   $m/z$  410.1379; found 411.1408 ( $\text{M}+\text{H}^+$ ).

**Chemosensor 3:** Yellow solid (280 mg, 83 %);  $R_f = 0.40$  (30% ethyl acetate:hexane);  $^1\text{H}$  NMR (500 MHz,  $\text{DMSO}-d_6$ )  $\delta$  14.89 (s, 1H), 9.64 (s, 1H), 9.22 (s, 1H), 8.56 (d, 1H,  $J = 8.5$  Hz), 8.01 (d, 1H,  $J = 9$  Hz), 7.95 (d, 1H,  $J = 7.5$  Hz), 7.87 (d, 1H,  $J = 8$  Hz), 7.58 (s, 2H), 7.48 (d, 2H,  $J = 7.5$  Hz), 7.40 (t, 1H,  $J = 7.5$  Hz), 7.31-7.27 (m, 3H), 7.20 (t, 1H,  $J = 7$  Hz), 7.15 (d, 1H,  $J = 9$  Hz), 6.98 (t, 1H,  $J = 7$  Hz);  $^{13}\text{C}$  NMR (125 MHz,  $\text{DMSO}-d_6$ ):  $\delta$  166.5, 159.3, 153.1, 140.2, 138.7, 136.6, 133.3, 132.6, 129.5, 129.3, 128.6, 127.5, 127.2, 124.3, 124.1, 122.6, 122.3, 121.2, 121.1, 120.2, 118.7, 110.1 ppm; HRMS (TOF MS ESI) calculated for  $\text{C}_{24}\text{H}_{19}\text{N}_3\text{O}_2$   $m/z$  381.1477; found 382.1548. ( $\text{M}+\text{H}^+$ ).



Scheme 1: Synthesis of chemosensors 1-6.

### 3. Results and Discussion

#### Spectroscopic comparison of chemosensors 1-3

The absorption spectrum of **1** in  $\text{CH}_3\text{CN}$  shows a broad absorption band centered at 337 nm due to internal charge transfer (ICT) across  $-\text{NH}$  fragment to the nitrophenyl group and a low energy shoulder band between 440-460 nm attributed to naphthol  $-\text{OH}$  moiety. The emission spectrum of **1** shows broad emission band centered at 458 nm, when excited at 330 nm, which is attributed to ESIPT process (Fig. 2).

Structurally compound **2** contains naphthyl instead of 2-hydroxynaphthyl group and it shows a broad absorption and

emission band centered at 327 nm and 411 nm, respectively. In case of compound **2**, the absorption band between 440-460 nm and ESIPT emission band at 458 nm belonging to hydroxyl naphthyl units are absent (Fig. 2). Chemosensor **3** contains phenyl urea instead of 4-nitrophenyl urea replacing electron withdrawing  $-\text{NO}_2$  group. The absorption spectrum of **3** shows two absorption bands centered at 315 and 380 nm due to internal charge transfer (ICT) across  $-\text{NH}$  fragment to phenyl and azomethine group transitions, respectively. A low energy shoulder band at 440-460 nm was also observed. In the emission spectrum, **3** shows broad ESIPT emission band at 458 nm, when excited at 330 nm (Fig. 2).

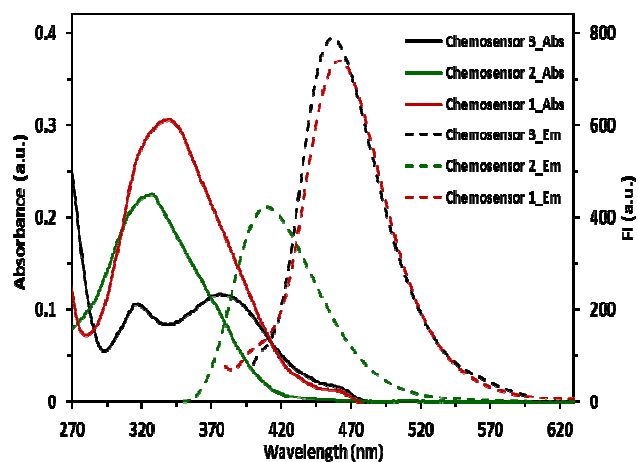


Fig. 2 Absorption and emission spectra of chemosensors 1-3 recorded in  $\text{CH}_3\text{CN}$ .

We have also recorded the absorption and emission spectra of the chemosensor **1** in various solvents and calculated the spectroscopic and photophysical properties (Fig. S1, table S2, ESI). The absorption maxima of **1** shows red shift of about 21 nm on changing the solvent from chloroform to acetonitrile to DMSO indicating charge transfer character in the ground state. We also observed that **1** shows maximum absorption intensity for de-protonation band (440 - 460 nm) in the polar protic solvents. Chemosensor **1** in non-polar solvents viz, ethyl acetate,  $\text{CH}_2\text{Cl}_2$ ,  $\text{CH}_3\text{CN}$ , dioxane gives emission at 458 nm due to ESIPT mechanism but in polar protic and aprotic solvents (DMF, ethanol, THF) ESIPT band is replaced by normal emission at 416 nm.

#### The response of chemosensor 1 to $\text{Cu}^{2+}$

The absorption spectrum of **1** ( $10 \mu\text{M}$ ,  $\text{CH}_3\text{CN}$ ) on addition of different metal perchlorates of  $\text{Na}^+$ ,  $\text{K}^+$ ,  $\text{Sr}^{2+}$ ,  $\text{Ba}^{2+}$ ,  $\text{Pb}^{2+}$ ,  $\text{Ni}^{2+}$ ,  $\text{Co}^{2+}$ ,  $\text{Fe}^{2+}$ ,  $\text{Zn}^{2+}$  ( $100 \mu\text{M}$ ) result in  $\sim 20\%$  decrease in absorbance intensity, however addition of  $100 \mu\text{M}$   $\text{Cu}^{2+}$  ions caused  $>50\%$  decrease along with concomitant blue shift of the absorption maxima. On gradual addition of  $\text{Cu}^{2+}$  ions, the intensity of absorption band at 337 nm was decreased with concomitant shift of the absorption band from 337 to 308 nm (blue shift  $\sim 29$  nm) up to addition of  $40 \mu\text{M}$  of  $\text{Cu}^{2+}$  ions and then attained the plateau (Fig. 3A). The colour of the solution changed from light yellow to colourless (Fig. 3A, Inset). The spectral fitting of these data using non-linear regression analysis shows the formation of 1:2 (L:M) stoichiometric complex with  $\log \beta_{\text{L}(\text{Cu}^{2+})} = 7.42 \pm 0.02$  (L: $\text{Cu}^{2+}$ , 1:2). The Job's

plot shows maxima at the mole fraction of 0.6 and confirms the formation of 1:2 (1-Cu<sup>2+</sup>) complex (Fig. S2, ESI).

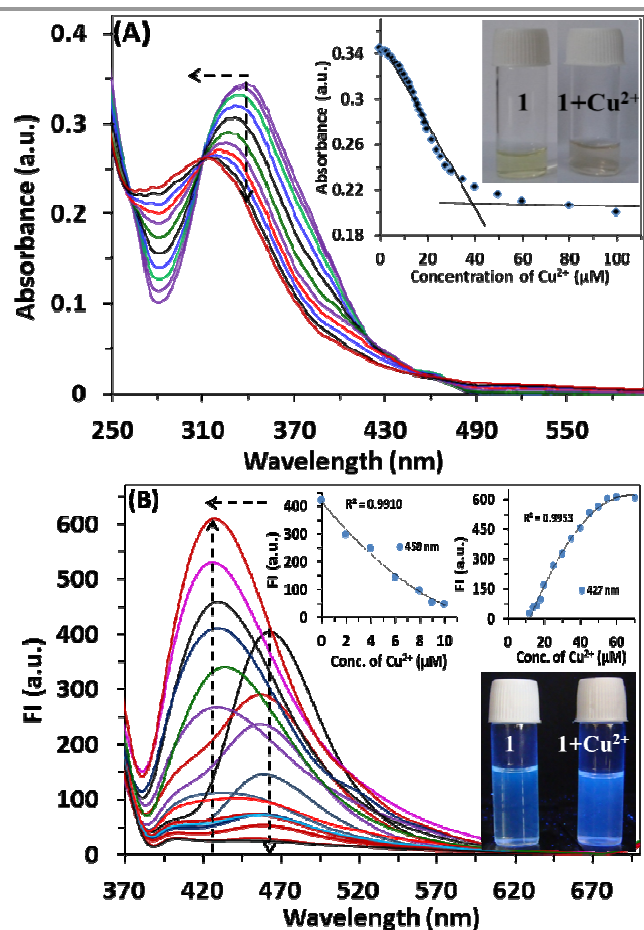


**Fig. 3** (A) UV-Vis spectra of **1** (10 μM) on addition of Cu<sup>2+</sup> ions. **Inset:** Plot of absorbance intensity vs conc. of Cu<sup>2+</sup> ions at 337 nm; Colour changes of **1** (10 μM) and **1** + Cu<sup>2+</sup> ions (40 μM). (B) Fluorescence spectra of **1** (10 μM) on addition of Cu<sup>2+</sup> ions; λ<sub>ex</sub> 330 nm, Slit width (Ex/Em = 10/20 nm). **Inset:** Plot of fluorescence intensity vs conc. of Cu<sup>2+</sup> ions at 458 and 427 nm; Fluorescence of **1** (10 μM) before and after addition of Cu<sup>2+</sup> ions (60 μM) under illumination at 365 nm.

When excited at 330 nm, chemosensor **1** showed fluorescence emission maxima at 458 nm and addition of 100 μM of Fe<sup>2+</sup>, Ba<sup>2+</sup>, Ni<sup>2+</sup>, Co<sup>2+</sup>, Zn<sup>2+</sup>, Sr<sup>2+</sup> and Pb<sup>2+</sup> caused 40% quenching of fluorescence intensity at 458 nm. The fluorescent titration of **1** (10 μM, CH<sub>3</sub>CN) with Cu<sup>2+</sup> showed that on gradual addition of Cu<sup>2+</sup> ions, the emission band at 458 nm was quenched up to addition of 1.0 equiv. (10 μM) of Cu<sup>2+</sup> ions and on further addition of Cu<sup>2+</sup> ions a new blue shifted emission band centered at 427 nm was observed whose intensity increased ~24 times up to 6.0 equiv. (60 μM) of Cu<sup>2+</sup> and then attained the plateau (Fig. 3B). So, chemosensor **1** behaves as ‘ON-OFF-ON’ molecular switch in the presence of Cu<sup>2+</sup> ions. The spectral fitting of these data using non-linear regression analysis shows the formation of 1:1 and 1:2 (L:M) stoichiometric complexes with log β<sub>L(Cu<sub>2</sub>)</sub> = 3.41 ± 0.2 (L:Cu<sup>2+</sup>, 1:1) and log β<sub>L(Cu<sub>2</sub>)</sub> = 6.78 ± 0.3 (L:Cu<sup>2+</sup>, 1:2).

In case of chemosensor **2** (10 μM) addition of even 100 μM concentration of Cu<sup>2+</sup> causes negligible blue shift (5 nm) in the absorption maxima as well as negligible fluorescence

quenching of the emission maxima (Fig. S3, ESI). On the other hand chemosensor **3**, on addition of Cu<sup>2+</sup> up to 200 μM shows decrease in absorption intensity at 380 nm. In the fluorescent titration of **3** with Cu<sup>2+</sup>, the emission band at 458 nm was quenched up to 1 equiv. of Cu<sup>2+</sup> ions and on further addition of Cu<sup>2+</sup> ions a new blue shifted emission band at 427 nm was observed whose intensity increased only 2 times up to 10.0 equiv. of Cu<sup>2+</sup> ions concentration (Fig. S4, ESI).

#### The response of chemosensor **1** to acetate and F<sup>-</sup> ions

The UV-Vis spectrum of **1** on addition of Cl<sup>-</sup>, Br<sup>-</sup>, ClO<sub>4</sub><sup>-</sup> and CN<sup>-</sup> remained silent. However, on addition of AcO<sup>-</sup> and F<sup>-</sup> ions to the solution of **1** the absorption band was red shifted from 337 nm to 360 nm, associated with H-bonding or deprotonation of -OH/-NH groups. The UV-Vis titration of **1** with AcO<sup>-</sup> ions shows ratiometric behavior up to 5.0 equiv. (50 μM) of AcO<sup>-</sup> ions, with isosbestic point at 349 nm (Fig. 4A).

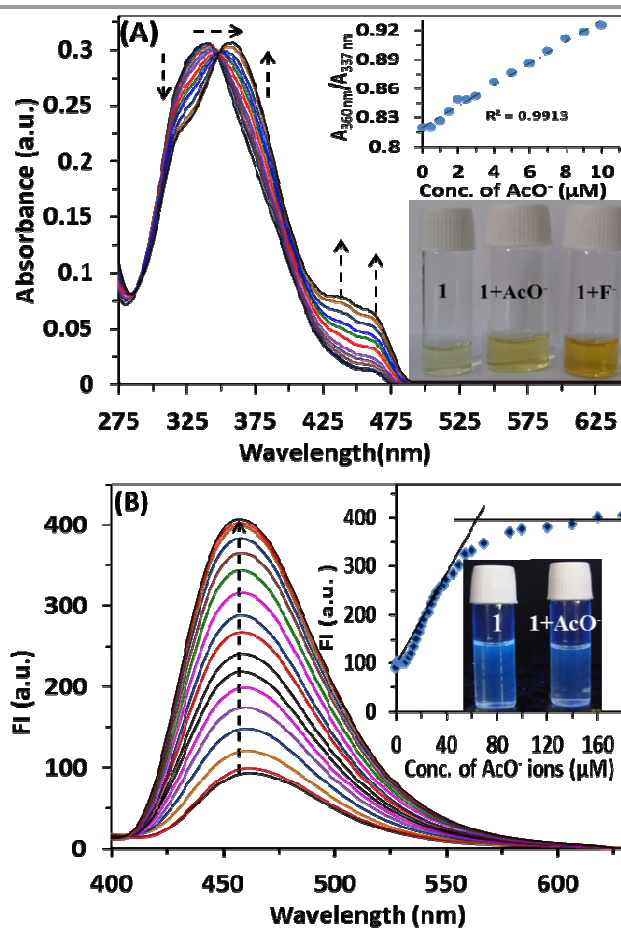


**Fig. 4** (A) UV-Vis spectra of **1** (10 μM) on addition of AcO<sup>-</sup> ions. **Inset:** Ratiometric plot of A<sub>360 nm</sub>/A<sub>337 nm</sub> vs conc. of AcO<sup>-</sup> ions; the colour changes of **1** (10 μM); **1** + AcO<sup>-</sup> ions (50 μM) and **1** + F<sup>-</sup> ions (50 μM). (B) Fluorescence spectra of **1** (10 μM) on addition of AcO<sup>-</sup> ions; λ<sub>ex</sub> 370 nm. Slit width (Ex/Em = 10 nm). **Inset:** Plot of fluorescence intensity vs conc. of AcO<sup>-</sup> ions; fluorescence of **1** (10 μM) before and after addition of AcO<sup>-</sup> ions (20 μM) under illumination at 365 nm.

The plot of ratios of absorbance intensities (A<sub>360nm</sub>/A<sub>337nm</sub>) vs. AcO<sup>-</sup> ions concentration shows a linear increase between 0-10 μM of AcO<sup>-</sup> ions (Fig. 4A, Inset). The spectral fitting of the

titration data shows the formation of 1:2 stoichiometric complex  $\log \beta_{L(OAc)} = 7.47 \pm 0.04$  (L:OAc, 1:2). The inflection point in Job's plot at the mole fraction of 0.7 further confirms the formation of 1:2 (1-AcO<sup>-</sup>) complex (Fig. S5, ESI).

On the other hand, addition of F<sup>-</sup> ions resulted in  $\lambda_{max}$  shift from 337 to 350 nm without ratiometric response along with band at 456 nm due to de-protonation of -OH moiety. The colour of the solution changed from light green to light yellow on addition of AcO<sup>-</sup> ions and dark yellow on addition of F<sup>-</sup> ions, (Fig. 4A, Inset).

The fluorescence titration of **1** in CH<sub>3</sub>CN against AcO<sup>-</sup> ions showed ~4 times increase in fluorescence intensity at 458 nm up to addition of 6 equiv. (60  $\mu$ M) of AcO<sup>-</sup> ions and thus constitutes fluorescence 'turn on' response at 458 nm. The spectral fitting of the titration data shows the formation of 1:2 stoichiometric complex  $\log \beta_{L(OAc)} = 7.17 \pm 0.02$  (L:OAc, 1:2). The inflection point in Job's plot at the mole fraction of 0.7 further confirms the formation of 1:2 (1-AcO<sup>-</sup>) complex. Similar results were also obtained with fluoride due to its higher basicity.

The control compounds **2** and **3** showed insignificant changes in their absorption and emission spectra on addition of acetate and F<sup>-</sup> ions (Fig. S6-7 ESI). These results clearly signify the presence of both nitro and -OH moieties essential for having the selective changes with Cu<sup>2+</sup>, AcO<sup>-</sup> and Cu(OAc)<sub>2</sub>.

#### The response of chemosensor **1** to Cu(OAc)<sub>2</sub> ion pair

In the light of above results, we expect that chromo-fluorescent sensor **1** possessing multiple binding sites should permit the simultaneous detection of Cu<sup>2+</sup> and AcO<sup>-</sup> ions. The UV-Vis titration of **1** (10  $\mu$ M) on incremental addition of solution of Cu(OAc)<sub>2</sub> up to 3 equiv. (30  $\mu$ M) concentration showed significant changes and then it achieved the plateau (Fig. 5). When we gradually added copper acetate, the absorption peak at 337 nm immediately started decreasing with concomitant appearance of blue shifted absorption band at 308 nm and red shifted absorption band at 380 nm. So, we attribute these absorption changes due to the apparent effect of Cu<sup>2+</sup> (blue shift, 337 to 308 nm in line with Cu<sup>2+</sup> titration with **1**) and AcO<sup>-</sup> (red shift, 337 to 360 nm in line with AcO<sup>-</sup> titration with **1**) as ion pair. The colour of the solution changed from light yellow to dark green (Fig. 5, Inset). In fluorometric titration of **1** with copper acetate, the fluorescence intensity at 458 nm increased 18 times up to addition of 1 equiv. of copper acetate, but blue-shift of the emission maxima is not observed. To achieve plateau, fewer quantity of Cu(OAc)<sub>2</sub> (3 equiv.) is required than individual Cu<sup>2+</sup> (6 equiv.) and AcO<sup>-</sup> (5 equiv.) ions.

As a proof of concept, we have also tested the sensing behavior of other ion pairs such as CuCl<sub>2</sub>, Cu(NO<sub>3</sub>)<sub>2</sub>, Pd(OAc)<sub>2</sub> and Hg(OAc)<sub>2</sub> towards chemosensor **1** in CH<sub>3</sub>CN. In case of these ion pairs, we observed either only increase in the absorption intensity at 337 nm without any spectral shift or only individual effect of Cu<sup>2+</sup> or acetate ions associated with de-protonation of -OH/-NH moiety (Fig. S8-9, ESI).

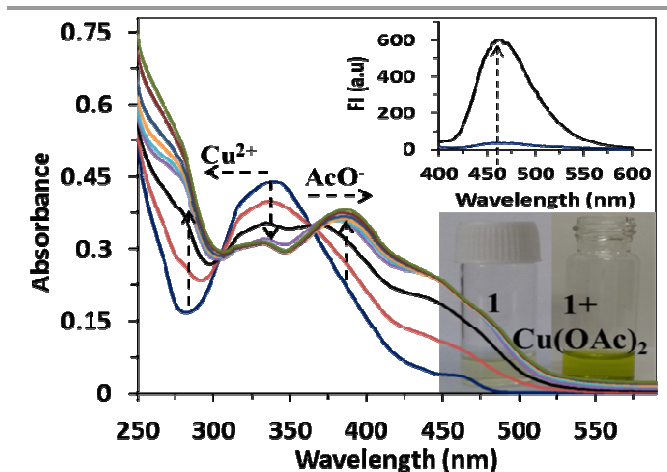


**Fig. 5** UV-Vis spectra of **1** (10  $\mu$ M) on addition of the Cu(OAc)<sub>2</sub> solution showing potential of **1** for simultaneous estimation of Cu<sup>2+</sup> and AcO<sup>-</sup> ions in the sample. **Inset:** fluorescence spectra of **1** (10  $\mu$ M) on addition of Cu(OAc)<sub>2</sub> (10  $\mu$ M);  $\lambda_{ex}$  370 nm. Slit width (Ex/Em = 10 nm); the colour changes of **1** (10  $\mu$ M); **1** + Cu(OAc)<sub>2</sub> (50  $\mu$ M).

To get more insight into our above concept of ion pair recognition, we also performed UV-Vis titration of (1:AcO<sup>-</sup>, 1:5) complex in the presence of different concentration of Cu<sup>2+</sup> ions. The UV-Vis spectrum of (1:AcO<sup>-</sup>, 1:5) complex showed red shifted absorption band at 360 nm in comparison to 337 nm for chemosensor **1** alone as discussed earlier. When we gradually added Cu<sup>2+</sup> to the (1:AcO<sup>-</sup>, 1:5) complex, the absorption peak shifted to 367 nm at 1 equiv. concentration of Cu<sup>2+</sup> ions (10  $\mu$ M), and on addition of 2 equiv. of Cu<sup>2+</sup> ions (20  $\mu$ M) the absorption band of **1** gradually shifted to 380 nm (Fig. 6). We also observed visually detectable solution colour change from light greenish to dark yellow (50  $\mu$ M conc. of AcO<sup>-</sup> ions) to dark green (up to 20  $\mu$ M conc. of Cu<sup>2+</sup> ions) (Fig. 6, Inset). However, when we performed the reverse titration i.e. gradual addition of acetate ions to the solution of (1:Cu<sup>2+</sup>, 1:4) complex, no such effect was observed (Fig. S10, ESI).

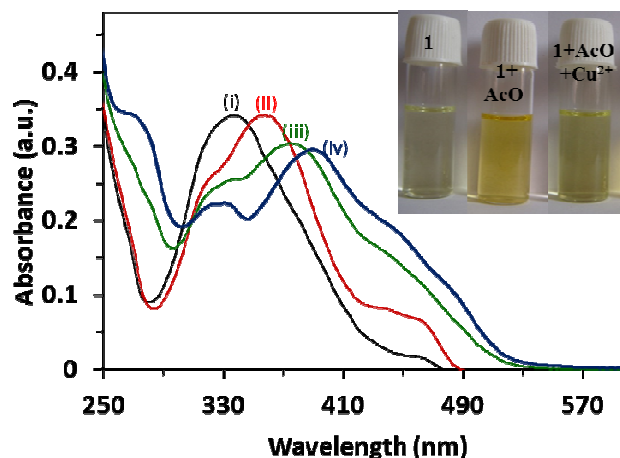


**Fig. 6** UV-Vis spectra of (1+AcO) complex on gradual addition of the Cu<sup>2+</sup> solution. (i) 10  $\mu$ M of **1**; (ii) 10  $\mu$ M of **1** and 50  $\mu$ M of acetate (iii) **1** + AcO<sup>-</sup> ions (50  $\mu$ M) + Cu<sup>2+</sup> ions (10  $\mu$ M) and (iv) **1** + AcO<sup>-</sup> ions (50  $\mu$ M) + Cu<sup>2+</sup> ions (20  $\mu$ M). **Inset:** The colour changes of **1** (10  $\mu$ M); **1** + AcO<sup>-</sup> ions (50  $\mu$ M) and **1** + AcO<sup>-</sup> ions (50  $\mu$ M) + Cu<sup>2+</sup> ions (20  $\mu$ M).

Similar UV-Vis titration of (1:F<sup>-</sup>, 1:5) complex in the presence of different concentration of Cu<sup>2+</sup> ions was performed. When we gradually added Cu<sup>2+</sup> to the (1:F<sup>-</sup>, 1:5) complex, the intensity of absorption peak at 356 nm decreases and on addition of higher concentration of Cu<sup>2+</sup> ions (100 μM) the absorption band of **1** gradually shifts from 356 to 320 nm (Fig. S11, ESI). Similarly, in the fluorescence titration of (1:F<sup>-</sup>, 1:5) complex, the addition of Cu<sup>2+</sup> causes only decrease in the emission intensity (Fig. S12, ESI). So, we conclude that the two different absorption outcomes could only be produced when both Cu<sup>2+</sup> and AcO<sup>-</sup> ions are simultaneously present in the solution.

The UV-Vis titration of control compounds **2** and **3** on addition of solution of copper acetate showed insignificant shift in their absorption bands (Fig. S13, ESI). So, we conclude that chemosensor **1** presents a unique example where we can monitor the sensing of Cu(OAc)<sub>2</sub> involving two different wavelengths simultaneously.

The selectivity towards Cu(OAc)<sub>2</sub> ion pair was further ascertained by the competition experiments where 300 μM of competing ion pairs were added to the 1-Cu(OAc)<sub>2</sub> (1:10) solution. As discussed earlier, the absorption spectrum of **1** on addition of Cu(OAc)<sub>2</sub> shows blue shift from 337 to 308 nm and red shift from 337 to 380 nm. On addition of 300 μM of various ion pairs did not cause any further spectral change in the absorption spectrum except increase in absorbance intensity at 290 nm due to absorbance of Cu<sup>2+</sup> itself at high concentration (Fig. S14, ESI).

#### Application as Logic Gates

As described above, the absorption and emission spectra of **1** are distinctively affected by the addition of Cu<sup>2+</sup> and acetate ions alone or simultaneously. It shows triple signaling with dual response for Cu<sup>2+</sup> (fluorescence 'turn on' response at 427 nm and fluorescence 'turn off' at 458 nm; colorimetric output at 308 nm; 'ON' and 337 nm; 'OFF') and acetate (fluorescence 'turn on' response at 458 nm; colorimetric output at 360 nm; 'ON' and 337 nm; 'OFF') ions individually as well as Cu(OAc)<sub>2</sub> ion pair (fluorescence 'turn on' response at 458 nm; colorimetric output at 380 nm; 'ON'). So, using Cu<sup>2+</sup> and acetate as inputs and absorption/fluorescence as output modes, the following logic gates could be fabricated (Fig. 6). Molecular switches and logic gates are analogues because both convert input stimulations into output signals with intrinsic protocols. In a positive logic convention, a 0 corresponds to the low output and 1 corresponds to high absorbance/emission output.

The compound **1** acts as an "ON-OFF-ON" switch driven by Cu<sup>2+</sup> with maximum fluorescence emission at 458 nm when [Cu<sup>2+</sup>] = 0 μM. The fluorescence falls off rapidly at 458 nm with addition of [Cu<sup>2+</sup>] = 10 μM and then reappears at different wavelength i.e. at 427 nm with [Cu<sup>2+</sup>] = 60 μM. So, it behaves as typical NOT gate at 458 nm and become Cu<sup>2+</sup> driven YES logic at 427 nm. Similarly, we also observe several NOT/YES logic gates for chemosensor **1** with different inputs at different wavelengths in the absorption mode such as NOT gate at 337 nm and YES gate at 308 nm on addition of Cu<sup>2+</sup> ions; NOT gate at 337 nm and YES gate at 360 nm on addition of acetate ions;

NOT gate at 337 nm and YES gate at 308 and 380 nm on addition of Cu(OAc)<sub>2</sub> ion pair.

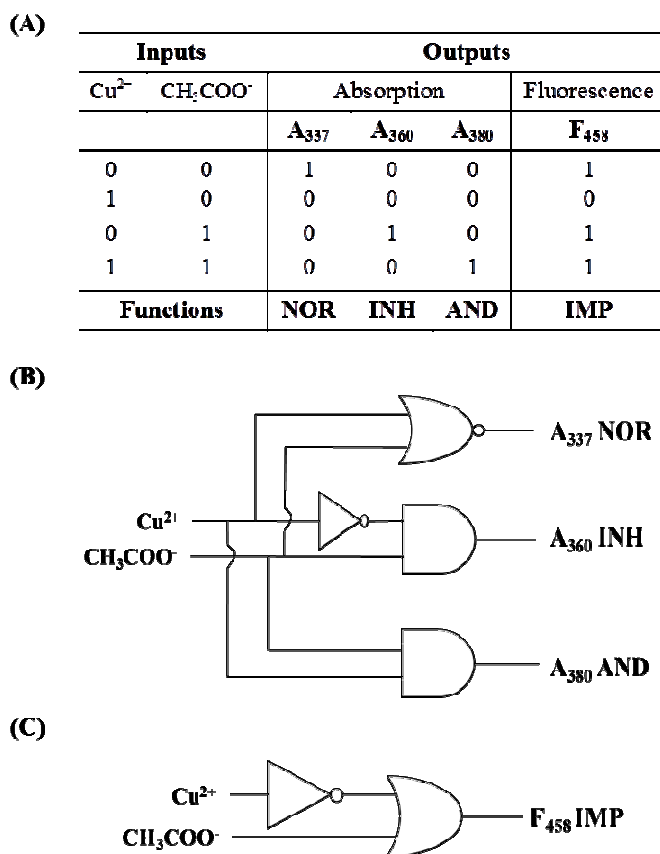


Fig. 7 (A) Truth table for various logic functions (NOR, AND, INH, IMP) fabricated for chemosensor **1** using Cu<sup>2+</sup> and acetate ions as inputs and absorption/emission as outputs at different wavelengths; (B) Pictorial representation of combinatorial circuit from NOR, INH and AND logic gate using absorption as output mode; (C) IMP logic gate using emission as output mode.

The pattern of absorption intensities as a function of cation and anion input read as a NOR logic function where absorption band at 337 nm in absence of both ions depicts 'on' state but as either or both of Cu<sup>2+</sup> and acetate ions are added, no absorption band centered at 337 nm exists that could be labelled as 'off' state (Fig. 7B). The other demonstration of molecular information processing was based on a photonic AND logic gate at A<sub>380</sub> nm. Absorbance at 380 nm could be at high value only when both inputs of Cu<sup>2+</sup> and acetate are simultaneously given to the system. When any one of the above two inputs is absent, the output will be in low state at A<sub>380</sub> nm (Fig. 7B).

An INHIBIT function is basically an AND operation where one input is reversed, i.e., in our case Cu<sup>2+</sup> ion in absorbance mode. The addition of acetate ions to the solution of **1** show output signal at 360 nm, however the presence of Cu<sup>2+</sup> inhibits the output signal caused due to acetate alone in the absorption mode and hence, INHIBIT (INH) function at A<sub>360</sub> nm was observed (Fig. 7B). Similar INH function was also observed at F<sub>427</sub> nm (fluorescence mode) where input of acetate ion is reversed.

The fluorescence output at 458 nm represents rarely reported IMPLICATION (IMP) logic gate. The IMPLICATION logic

gate is equivalent to an OR gate except one of its two input lines contains an inversion operation. At  $F_{458}$  wavelength, the output value is in low state only when  $\text{Cu}^{2+}$  is introduced into the system. Otherwise, the output at 458 nm is in high state (Fig. 7C).

### $^1\text{H}$ NMR Titration Studies

The interaction of sensor **1** with tetrabutylammonium acetate, copper perchlorate and copper acetate were also probed through  $^1\text{H}$  NMR titration however due to poor solubility of chemosensor **1** (5 mM) in  $\text{CD}_3\text{CN}$ , we prefer  $\text{DMSO}-d_6$  solvent for  $^1\text{H}$  NMR titrations. The  $^1\text{H}$  NMR spectrum of the sensor **1** showed signals at  $\delta$  9.93 ppm and  $\delta$  9.64 ppm due to  $-\text{NH}$  protons of urea moiety. The signals at  $\delta$  14.88 ppm and  $\delta$  8.56 ppm correspond to  $-\text{OH}$  group and imine proton ( $\text{CH}=\text{N}$ ), respectively. We observed that the proton signal of the naphthol hydroxyl group at  $\delta$  14.88 ppm and proton signal of the  $-\text{NH}$  group attached to p-nitrophenyl at  $\delta$  9.93 ppm disappeared (due to fast exchange of H-bond on NMR time scale) on addition of 1.0 equiv of acetate ions along with 0.12 ppm up field shift of the remaining  $-\text{NH}$  proton signal. Moreover we also observed up-field chemical shift of the naphthalene aromatic protons on addition of acetate ions (Fig. 8).

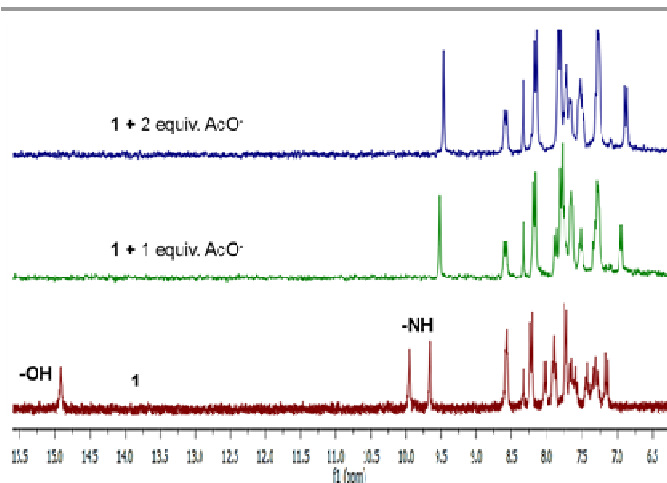


Fig. 8 Partial  $^1\text{H}$  NMR spectrum of chromo-fluorescent sensor **1** recorded in  $\text{DMSO}-d_6$  at different addition (in equivalent) of (A) tetrabutylammonium acetate

In case of  $^1\text{H}$  NMR titration of chemosensor **1** with  $\text{Cu}(\text{ClO}_4)_2$ , we observed decrease in the intensity for peak corresponding to  $-\text{OH}$  group which again indicates H-bonding or de-protonation mechanism. Moreover Schiff base proton and urea  $-\text{NH}$  protons underwent very small shift which indicate weak complexation of urea  $-\text{NH}$  with  $\text{Cu}^{2+}$  ions. However in case of  $^1\text{H}$  NMR titration of chemosensor **1** with  $\text{Cu}(\text{AcO})_2$  we observed decrease in intensity for both  $-\text{OH}$  and  $-\text{NH}$  protons indicating complexation of ion pair at their respective binding site (see Fig. S15, ESI).

### Structure optimization using DFT

Geometries of chemosensor **1** and its 1:1 adducts with  $\text{Cu}^{2+}$ ,  $\text{AcO}^-$  and  $\text{Cu}(\text{OAc})_2$  ion pair, respectively were also fully optimized with B3LYP functional and 6-31G\* basis set. Firstly, the two possible conformations of **1** were optimized using B3LYP (6-31G\*) basis set. The energy of conformation 'B' was found to be more stable than conformation 'A' by only

6.53 kcal/mol (Fig. 9). So, there is a dynamic equilibrium between these two conformations and molecule can attain either of two conformations. The optimized structure of **1** shows *anti* geometry of the urea group and we could expect cleft-like geometry which provides perfect platform for O- and N- atoms of Schiff base chelating group and carbonyl group of urea to coordinates with cation and  $-\text{NH}$  of urea to coordinate with anion.

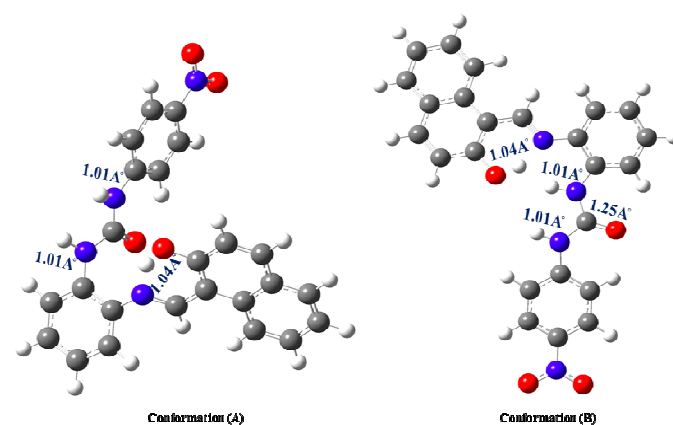


Fig. 9 The energy minimized structures (DFT 6-31G\*) of chemosensor **1**.

The optimized structure of **1**- $\text{Cu}^{2+}$  complex shows participation of three donor atoms i.e.,  $\text{C}=\text{O}$ ,  $-\text{OH}$  and  $\text{C}=\text{N}$  towards  $\text{Cu}^{2+}$  with bonding distance 1.87, 1.79 and 1.87 Å, respectively. The optimized structure of **1**- $\text{AcO}^-$  (1:2) complex showed participation of  $\text{AcO}^-$  ions in H-bonding with  $-\text{OH}$  of naphthol and  $-\text{NH}$  of urea group (Fig. 10).

The **1**- $\text{AcO}^-$  complex was found to be more stable by 55.01 kcal/mol in comparison to **1(A)**. For complex **1**- $\text{AcO}^-$ , the optimized distances between acetate and two  $-\text{NH}$  group were calculated to be 1.77 and 1.70 Å. The second acetate binds with **1** through  $-\text{OH}$  of naphthol. The binding of acetate also caused elongation of  $-\text{NH}$  bond of urea by 0.039 and 0.031 Å and  $-\text{OH}$  bond by 0.30 Å as compared with conformation **1(A)**.

To study the effect of ion pair, similar studies were conducted using **1**- $\text{Cu}(\text{OAc})_2$  complex. The optimized structure of **1** with  $\text{Cu}(\text{OAc})_2$  ion pair shows simultaneous complexation of three donor atoms ( $\text{C}=\text{O}$ ,  $-\text{OH}$ ,  $\text{C}=\text{N}$ ) towards  $\text{Cu}^{2+}$  with bonding distance 1.84, 1.81 and 1.87 Å, respectively, and complexation of  $-\text{NH}$  group of urea with acetate with bonding distance of 1.53 and 1.55 Å.

The **1**- $\text{Cu}(\text{OAc})_2$  also showed elongation of  $-\text{C}=\text{O}$  bond by 0.027 Å when compared with conformation **1(A)**. This complex also showed elongation of  $-\text{NH}$  bond of urea by 0.080 and 0.069 Å as compared with conformation **1(A)**. The **1**- $\text{Cu}^{2+}$  complex was found to be more stable by 135.28 kcal/mol in comparison to **1(A)**. So, **1**- $\text{Cu}^{2+}$  complex was found to be more stable in compare to **1**- $\text{AcO}^-$  complex and thus provides evidence for displacement of  $\text{AcO}^-$  ions on gradual addition of  $\text{Cu}^{2+}$  ions to the **1**- $\text{AcO}^-$  solution (discussed above).

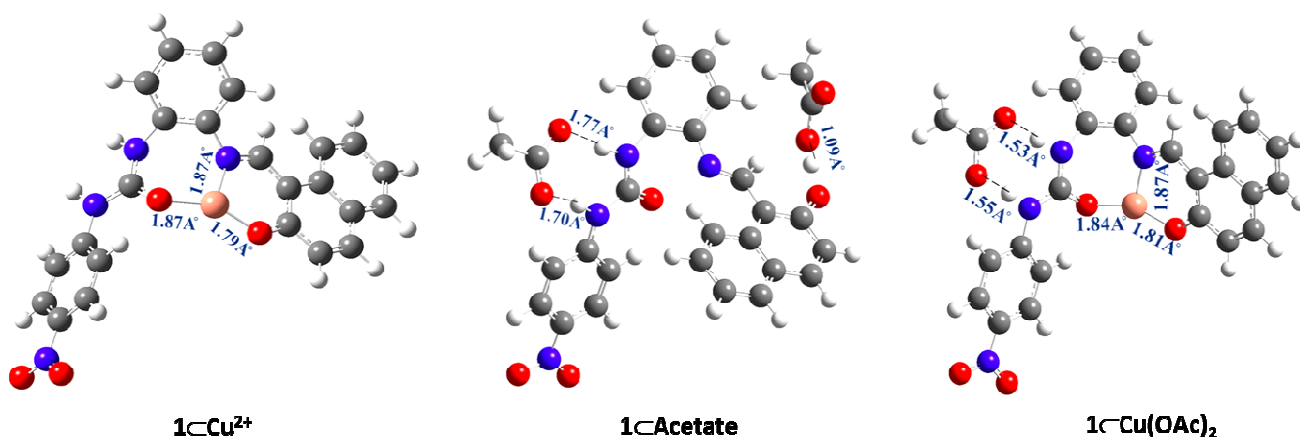


Fig. 10 The energy minimized structures (DFT 6-31G\*) of  $\text{Cu}^{2+}$  ( $1\text{Cu}^{2+}$ ),  $\text{AcO}^-$  ( $1\text{Acetate}$ ) and  $[1\text{Cu}(\text{OAc})_2]$  complex.

### Proposed mechanism for complexation

Mechanistically, we propose that one  $\text{Cu}^{2+}$  ion coordinates with Schiff base and with urea moiety of chemosensor **1** and thus inhibits the ICT from urea nitrogen to electron deficient *p*-nitrophenyl causing blue-shift of  $\lambda_{\text{max}}$  from 337 to 308 nm along with decrease in absorption intensity due to binding of C=N of azomethine and -OH of hydroxynaphthyl with  $\text{Cu}^{2+}$  ions. In fluorescence spectrum of chemosensor **1**, the addition of 1 equiv. of  $\text{Cu}^{2+}$  inhibited ESIPT band at 458 nm due to binding with -OH. Further addition of  $\text{Cu}^{2+}$  ions, resulted in release of normal emission of naphthalenoxy moiety supplemented due to restriction in rotation in imine (C=N) moiety (Fig. 11). Lack of -OH in chemosensor **2**, reduced significantly the copper complexation as observed in UV-Vis and fluorescence titrations. Similarly, absence of -NO<sub>2</sub> group in chemosensor **3**, resulted in weak ICT mechanism and no blue shift on addition of  $\text{Cu}^{2+}$ .

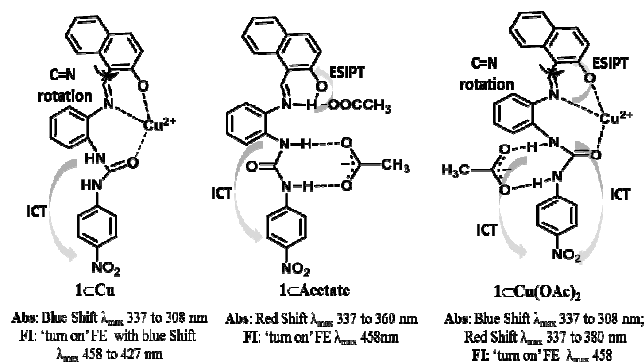


Fig. 11 Proposed binding modes of chromo-fluorescent sensor **1** with  $\text{AcO}^-$ ,  $\text{Cu}^{2+}$  and  $\text{Cu}(\text{OAc})_2$  salt showing different modulation of ICT, ESIPT and C=N rotation channel.

When acetate ions were added to the solution of chemosensor **1**, one  $\text{AcO}^-$  ion coordinated with -NH groups of nitrophenylurea, and increase ICT between electron rich anion bound urea and electron deficient *p*-nitrophenyl moiety with red-shift of  $\lambda_{\text{max}}$  from 337 to 360 nm. The second acetate molecule coordinates with naphthyl -OH group and caused

increase in fluorescence intensity at 458 nm (ESIPT) phenomena (Fig. 11). The lack of -OH group in chemosensor **2** resulted in no fluorescence enhancement on addition of  $\text{AcO}^-$  ions.

When  $\text{Cu}(\text{OAc})_2$  was added for simultaneous estimation of both ions, the individual ions coordinated with the respective binding sites. However, the increased red-shift of 337 nm band to 380 nm on addition of  $\text{Cu}(\text{OAc})_2$  as compared to 337 to 360 nm in case of  $\text{AcO}^-$  alone is attributed to the synergistic effect of both  $\text{Cu}^{2+}$  and  $\text{AcO}^-$  on each other's binding. Probably, simultaneous binding of  $\text{Cu}^{2+}$  with carbonyl oxygen as depicted in figure 11 increases the acidity of urea group and results in enhanced ICT on binding with acetate. This fact was proved on titration of  $(1+\text{AcO}^-)$  complex on addition of  $\text{Cu}^{2+}$  ions where the  $\lambda_{\text{max}}$  first shift from 360 to 380 nm as discussed earlier. Probably, this mode of  $\text{Cu}^{2+}$  binding is also responsible for the observed blue shift in the absorption spectrum of **1** when  $\text{Cu}(\text{OAc})_2$  was added.

### Conclusion

In summary, we have synthesized chromo-fluorescent chemosensor **1** that possesses Schiff base and urea moieties as dual binding sites for recognition of  $\text{Cu}^{2+}$ ,  $\text{AcO}^-$  ions and  $\text{Cu}(\text{OAc})_2$  ion pair. In coherence participation of internal charge transfer, ESIPT and restriction in rotation of C=N bond phenomena have been responsible for the observed absorbance/fluorescence changes in the presence of  $\text{Cu}^{2+}$ ,  $\text{AcO}^-$  and both. We have also demonstrated the potential application of chemosensor **1** for construction of INH, IMP, AND, NOR, YES and NOT logic gates operated by  $\text{Cu}^{2+}$  and acetate as inputs and absorbance/emission as outputs.

### Acknowledgements

This work was supported by UGC grant for newly recruited faculty, CSIR (Grant No. 02(0084)/12/EMR-II) and UPE programmes. H.S. is thankful to the UGC for the research fellowship under UPE programme.

## Notes and References

1. J. Janata, (Guest Ed.) Special issue on Modern Topics in Chemical Sciences, *Chem. Rev.*, 2008, **108**, 327.
2. J. Wu, W. Liu, J. Ge, H. Zhang and P. Wang, *Chem. Soc. Rev.*, 2011, **40**, 3483.
3. (a) K. Kaur, R. Saini, A. Kumar, V. Luxami, N. Kaur, P. Singh and S. Kumar, *Coord. Chem. Rev.*, 2012, **256**, 1992; (b) M. Formica, V. Fusi, L. Giorgi and M. Micheloni, *Coord. Chem. Rev.*, 2012, **256**, 170; (c) J. F. Zhang, Y. Zhou, J. Yoon and J. S. Kim, *Chem. Soc. Rev.*, 2011, **40**, 3416.
4. (a) Q. Hu, Y. Liu, Z. Li, R. Wen, Y. Gao, Y. Bei and Q. Zhu, *Tetrahedron Lett.* 2014, **55**, 4912; (b) M. Shellaiah, Y.-H. Wu, A. Singh, M. V. R. Raju and H.-C. Lin, *J. Mater. Chem. A* 2013, **1**, 1310; (c) R. Martinez, A. Espinosa, A. Tarraga and P. Molina, *Org. Lett.* 2005, **7**, 5869; (d) S. Wang, G. Men, L. Zhao, Q. Hou and S. Jiang, *Sensors and Actuators, B: Chemical* 2010, **145**, 826.
5. (a) S. Goswami, S. Paul and A. Manna, *RSC Advances*, 2013, **3**, 25079; (b) D. Maity and T. Govindaraju, *Chem. Commun.*, 2012, **48**, 1039.
6. (a) P. Das, A. Ghosh, H. Bhatt and A. Das, *RSC Advances*, 2012, **2**, 3714; (b) X. Li, M. Yu, F. Yang, X. Liu, L. Wei and Z. Li, *New J. Chem.*, 2013, **37**, 2257.
7. (a) L. Ding, M. Wu, Y. Li, Y. Chen and J. Su, *Tetrahedron Lett.*, 2014, **55**, 4711; (b) S. Devaraj, D. Saravanakumar and M. Kandaswamy, *Sensors and Actuators, B: Chemical*, 2009, **136**, 13; (c) M. A. Kaloo and J. Sankar, *New J. Chem.*, 2014, **38**, 923.
8. S. Goswami, S. Maity, A.K. Das and A.C. Maity, *Tetrahedron Lett.*, 2013, **54**, 6631.
9. V. Garcia, A. Fernandez-Lodeiro, R. Lamelas, A. Macias, R. Bastida, E. Bertolo and C. Nunez, *Dyes Pigments* 2014, **110**, 143.
10. (a) J. G. Jung, M. Kang, J. Chun, J. Lee, J. Kim, J. Kim, Y. Kim, S. J. Kim, C. Lee and J. Yoon, *Chem. Commun.* 2013, **49**, 176; (b) Q. Xu, K. M. Lee, F. Wang and J. Yoon, *J. Mater. Chem.* 2011, **21**, 15214; (c) A.-F. Li, J.-H. Wang, F. Wang and Y.-B. Jiang, *Chem. Soc. Rev.*, 2010, **39**, 3729; (d) T. Gunnlaugsson, M. Glynn, G. M. Tocci (nee Hussey), P. E. Kruger and F. M. Pfeffer, *Coord. Chem. Rev.*, 2006, **250**, 3094.
11. (a) A. Okudan, S. Erdemir and O. Kocyigit, *J. Mol. Structure*, 2013, **1048**, 392; (b) H. Su, W. Huang, Z. Yang, H. Lin and H. Lin, *J. Incl. Phenom. Macrocycl. Chem.*, 2012, **72**, 221.
12. (a) D. Maity and T. Govindaraju, *Eur. J. Inorg. Chem.* 2011, **20**, 5479; (b) D. Maity, A. K. Manna, D. Karthigeyan, T. K. Kundu, S. K. Pati and T. Govindaraju, *Chem. Eur. J.* 2011, **17**, 11152;
13. (a) S. Goswami, A.K. Das, D. Sen, K. Aich, H.-K. Fun and C.K. Quah, *Tetrahedron Lett.*, 2012, **53**, 4819; (b) Y.-G. Zhang, Z.-H. Shi, L.-Z. Yang, X.-L. Tang, Y.-Q. An, Z.-H. Ju and W.-S. Liu, *Inorg. Chem. Commun.*, 2014, **39**, 86.
14. (a) M. Bonizzoni, L. Fabbrizzi, A. Taglietti and F. Tiengo, *Eur. J. Org. Chem.*, 2006, 3567; (b) Y.-J. Kim, H. Kwak, S. J. Lee, J. S. Lee, H. J. Kwon, S. H. Nam, K. Lee and C. Kimb, *Tetrahedron*, 2006, **62**, 9635.
15. (a) Z.-C. Wen, R. Yang, H. He and Y.-B. Jiang, *Chem. Commun.* 2006, 106; (b) S. Kumar, P. Singh and S. Kaur, *Tetrahedron* 2007, **63**, 11724.
16. (a) Stern, B. R. *J. Toxicol. Environ. Health Part A: Current Issues*, 2010, **73**, 114; (b) G. Crisponi, V. M. Nurchi, D. Fanni, C. Gerosa, S. Nemolato and G. Faa, *Coord. Chem. Rev.*, 2010, **254**, 876.
17. F. P. Schmidtchen and M. Berger, *Chem. Rev.*, 1997, **97**, 1609.
18. A. P. de silva, H. Q. Nimal Gunaratne and C. P. McCoy, *Nature*, 1993, **364**, 42.
19. (a) A. P. de Silva, *Chem. Asian J.*, 2011, **6**, 750; (b) X. Zhou, X. Wu and J. Yoon, *Chem. Commun.* 2015, **51**, 111.
20. (a) K. Szacilowski, *Chem. Rev.*, 2008, **108**, 3481; (b) S. Kou, H. N. Lee, D. V. Noort, K. M. K. Swamy, S. H. Kim, J. H. Soh, K. M. Lee, S. W. Nam, J. Yoon and S. Park, *Angew Chem. Int. Ed.* 2008, **47**, 872.
21. (a) A. P. de Silva, N. D. McClenaghan, *Chem. Eur. J.*, 2004, **10**, 574; (b) A. P. de Silva and S. Uchiyama, *Nat. Nanotech.*, 2007, **2**, 399
22. T. Gupta, M. E. van der Boom, *Angew. Chem. Int. Ed.*, 2008, **47**, 5322.
23. (a) U. Pischel, B. Heller, *New J. Chem.*, 2008, **32**, 395; (b) U. Pischel, *Angew. Chem. Int. Ed.*, 2007, **46**, 4026.
24. S. Kumar, V. Luxami, R. Saini and D. Kaur, *Chem. Commun.*, 2009, 3044.
25. (a) D. Margulies, G. Melman and A. Shanzer, *J. Am. Chem. Soc.*, 2006, **128**, 4865; (b) D. Margulies, G. Melman and A. Shanzer, *Nature Materials*, 2005, **4**, 768.
26. (a) P. Singh and S. Kumar, *New J. Chem.*, 2006, **30**, 1553; (b) P. Singh and S. Kumar, *Tetrahedron*, 2007, **62**, 6379; (c) P. Singh and S. Kumar, *Tetrahedron Lett.*, 2006, **47**, 109.
27. P. Singh, R. Kumar and S. Kumar, *J. Fluoresc.* 2014, **24**, 417.
28. P. Singh, L.S. Mittal, S. Kumar, G. Bhargava and S. Kumar, *J. Fluoresc.* 2014, **24**, 909.
29. (a) K. Ghosh and I. Saha, *Org. Biomol. Chem.*, 2012, **10**, 9383; (b) K. Ghosh and I. Saha, *New J. Chem.*, 2011, **35**, 1397.
30. (a) T.S. Singh, P.C. Paul, H.A.R. Pramanik, *Spectrochimica Acta, Part A: Mol. Biomol. Spect.*, 2014, **121**, 520; (b) K. Ghosh, I. Saha and A. Patra, *Tetrahedron Lett.*, 2009, **50**, 2392.
31. W. Jiamin, L. Shaoguang, Y. Peiju, H. Xiaojuan, J.Y. Xiao and W. Biao, *CrystEngComm.*, 2013, **15**, 4540.
32. M. Sahin, N. Kocak, D. Erdenay and U. Arslan, *Spectrochimica Acta, Part A: Mol. Biomol. Spect.*, 2013, **103**, 400.

# Triple-signaling mechanisms-based three-in-one multi-channel chemosensor for discriminating $\text{Cu}^{2+}$ , acetate and ion pair mimicking AND, NOR, INH and IMP logic functions

Prabhpreet Singh<sup>a,\*</sup>, Harminder Singh<sup>a</sup>, Gaurav Bhargava<sup>b</sup> and Subodh Kumar<sup>a</sup>

<sup>a</sup>Department of Chemistry, UGC Centre for Advanced Studies, Guru Nanak Dev University, Amritsar 143 005, India.

e-mail: prabhpreet.chem@gndu.ac.in; Tel: +91-84271-01534

<sup>b</sup>Department of Applied Sciences, Punjab Technical University, Kapurthala-144601, Punjab, India.

Chemosensor **1** shows three different responses towards  $\text{Cu}^{2+}$ , acetate and  $\text{Cu}(\text{OAc})_2$  ion pair at different wavelengths independently, following triple-signaling mechanisms (ICT, C=N rotation and ESIPT) and also demonstrate fabrication of INH, IMP, AND, NOR, YES and NOT logic gates.

